Talanta 150 (2016) 661–665

Contents lists available at ScienceDirect

Talanta

journal homepage: www.elsevier.com/locate/talanta

Dendritic DNA–porphyrin as mimetic enzyme for amplified fluorescent detection of DNA

Nan Xu, Jianping Lei *, Quanbo Wang, Qianhui Yang, Huangxian Ju

State Key Laboratory of Analytical Chemistry for Life Science, School of Chemistry and Chemical Engineering, Nanjing University, Nanjing 210093, PR China

ARTICLE INFO

Article history:
Received 17 August 2015
Received in revised form
24 December 2015
Accepted 3 January 2016
Available online 4 January 2016

Keywords:
Porphyrin
Mimetic enzyme
Fluorescent assay
Dendritic superstructure
DNA detection

ABSTRACT

In this work, a novel dendritic DNA–porphyrin superstructure was designed as mimetic enzyme for the amplified fluorescent detection of DNA. The dendritic DNA superstructure was in situ assembled with three auxiliary DNAs via hybridization chain reaction. With groove interaction between iron porphyrin (FeTMPyP) and double-stranded DNA, the dendritic DNA superstructure is capable to gather abundant FeTMPyP molecules to form dendritic DNA–FeTMPyP mimetic enzyme. Using tyramine as a substrate, the dendritic DNA–FeTMPyP demonstrated excellent peroxidase-like catalytic oxidation of tyramine into fluorescent dityramine in the presence of H_2O_2. Based on an amplified fluorescence signal, a signal on strategy is proposed for DNA detection with high sensitivity, good specificity and practicability. The assembly of porphyrin with dendritic DNA not only provided the new avenue to construct mimetic enzyme but also established label-free sensing platform for a wide range of analytes.

1. Introduction

The sensitive detection of DNA fragment is urgently required in genic analysis and clinical diagnosis. To improve the sensitivity, the most feasible pathway is to transduce a one-target recognition event to multiple signal molecules by incorporating multiple signal probes into the detection system. Hybridization chain reaction (HCR) acts as a kind of nonenzyme-assisted nucleic acid amplification technology, which causes oligonucleotides to polymerize spontaneously into long double-stranded DNA (dsDNA) [1]. The HCR-based signal amplification method has been successfully applied to the construction of fluorescent [2–4], electrochemiluminescent [5,6] and electrochemical biosensors with high sensitivity and good specificity [7,8]. Xia and co-workers designed a supersandwich DNA structure by alternately hybridizing target DNA with signal probe to capture multiple methylene blue molecules for electrochemical signal amplification [9]. However, the construction of the supersandwich structure involved many target DNA, which limited the detection sensitivity. To further improve the sensitivity of electrochemical DNA detection, Chen et al. utilized one target to initiate the assembly of long DNA concatamer to electrode with auxiliary DNA [10,11]. In this work, a single target DNA was employed as initiator to assemble a dendritic DNA superstructure to immobilize porphyrin for signal amplification.

Iron porphyrin owns excellent catalytic activity and could simulate horseradish peroxidase (HRP) and peroxidase to catalyze multiple oxidation reactions [12–15]. However, the self-aggregation of free iron porphyrin molecule in the solution could weaken its catalytic activity and simultaneously limit the further application [16,17]. Fortunately, iron(III) meso-tetrakis(N-methylpyridinum-4-yl) porphyrin (FeTMPyP) molecules have been reported to interact with AT and GC base pairs of dsDNA, and thus are embedded into the groove of dsDNA [18–21]. The integrating FeTMPyP molecule with dsDNA could effectively avoid the self-aggregation phenomenon and improve its catalytic performance. Compared with the natural proteases such as HRP [22,23], glucose oxidase [24,25], exonuclease [26–28] and endonuclease [29–31], DNA–FeTMPyP owns excellent biomimetic catalytic activity with simpler preparation, easier modification and especially better stability. It is worth noting that the length of dsDNA determines the capacity of FeTMPyP molecules and directly affects the catalytic activity of DNA–FeTMPyP. Zang and co-workers used catalytic hairpin assembly reaction to design FeTMPyP@dsDNA with high catalytic activity for photoelectrochemical biosensing [32]. This method could effectively improve the sensitivity of the photoelectrochemical strategy, but required complex and precise design of hairpin DNA sequences. Recently, the covalent DNA-linked hemin probes were designed for homogenous DNA sensing strategy based on the inhibition effect of peroxidase activity by graphene oxide or dual-hemin with the sub-nanomolar detection limit [33,34]. In order to further improve the catalytic performance of DNA–FeTMPyP and simplify the DNA sequences simultaneously, we integrated the advantages of HCR and FeTMPyP to design a dendritic DNA–FeTMPyP mimetic enzyme for fluorescent

* Corresponding author.
E-mail address: jpl@nju.edu.cn (J. Lei).

http://dx.doi.org/10.1016/j.talanta.2016.01.005
0039-9140/

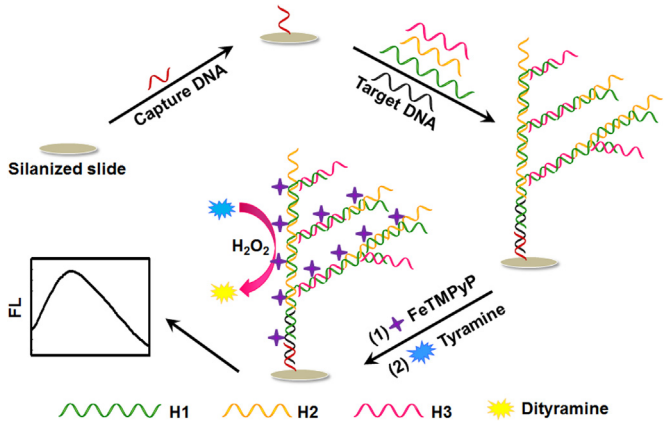

Fig. 1. Schematic illustration of in situ assembly of a dendritic DNA–FeTMPyP as mimetic enzyme for amplified fluorescent detection of DNA.

detection of DNA without requirement of complex sequences.

Here, we designed a HCR-based dendritic DNA–FeTMPyP as mimetic enzyme and utilized tyramine as substrate to develop an amplified fluorescence strategy for DNA detection (Fig. 1). With target DNA (TD) as linker and capture DNA (CP) as capturer, three kinds of auxiliary DNA participated in hybridization chain reaction and finally the gigantic dendritic DNA structure was in situ assembled onto the modified slide. By the groove interaction of FeTMPyP with dsDNA, abundant catalytic FeTMPyP molecules were caught into dendritic DNA structure and thus dendritic DNA–FeTMPyP as mimetic enzyme was successfully constructed to in situ catalytically oxidize tyramine into fluorescent dityramine. The enhanced fluorescence signal resulted in sensitive fluorescence method for target DNA detection. The novel dendritic DNA–FeTMPyP as mimetic enzyme with excellent catalytic activity could be simply prepared without need of complex and complicated sequence, showing a promising application in practice.

2. Experimental

2.1. Materials and reagents

All oligonucleotides were synthesized and HPLC-purified by Sangon Biological Engineering Technology & Co. Ltd. (Shanghai, China). Their sequences were as follows:

CP: 5′-CAGTGTGGAAAATCTCTAGC-$(CH_2)_7$-NH_2-3′
TD: 5′-GCTAGAGATTTTCCACACTGACTAAAAGGGTCTGAGGG-3′
Help DNA 1 (H1): 5′-TCACGACGACGATCATCT*CATACTCCCCCAGGTGC*CCC TCAGACCCTTTTAGT-3′
Help DNA 2 (H2): 5′-*GCACCTGGGGGAGTATG*ACTAAAAGGGTCTGAGGG-3′
Help DNA 3 (H3): 5′-AGATGATCGTCGTCGTGAACTAAAAGGGTCTGA GGG-3′
smT: 5′-GCTAGAGATTTT*G*CACACTGACTAAAAGGGTCTGAGGG-3′
tmT: 5′-GCTAGA*C*ATTTT*G*CACA*G*TGACTAAAAGGGTCTGAGGG-3′
ncT: 5′-GGATCAGATAATCGAGACTCACTAAAAGGGTCTGAGGG-3′

Here, mismatched bases are highlighted in blue italic type.

The slide was purchased from Zhuhai Kaivo Electronic Components Co. Ltd. (China). 3-Glycidyloxypropyl trimethoxysilane (GOPS) and tyramine were purchased from Sigma-Aldrich (Shanghai) Trading Co. Ltd. FeTMPyP was a gift from Kanazawa University (Japan). All other reagents were of analytical reagent grade and used as purchased without further purification. Phosphate buffer saline (PBS) (10 mM, containing 137 mM NaCl, 2.7 mM $MgCl_2$ and 10 mM ethanolamine, pH 7.4) was used to block the slide. Tris–HCl buffer (10 mM, containing 100 mM NaCl, pH 7.4) was used for fluorescent measurements. Human blood serum samples were obtained from Jiangsu Province Tumor Hospital (Nanjing, China). Ultrapure water obtained from a Millipore water purification system (≥ 18 MΩ, Milli-Q, Millipore) was used in all experiments.

2.2. Apparatus

Gel electrophoresis analysis was conducted on the DYCP-31 BN electrophoresis analyzer (Liuyi Instrument Company, China) and imaged on the Biorad ChemDoc XRS (USA). Circular Dichroism (CD) spectra were obtained by Chirascan circular dichroism spectrometer (England) and the lamp was always kept under a stable stream of drypurified nitrogen (99.99%) during experiments. The fluorescence spectra were recorded from 370 to 500 nm with a step of 1 nm at the excitation wavelength of 320 nm on a RF-5301 PC spectrofluorometer (Shimadzu Co., Japan) equipped with a xenon lamp. The excitation slit width was 10 nm, and the emission slit width was 5 nm.

2.3. Gel electrophoresis

DNA was annealed by heating at 92 °C for 10 min and gradually cooling to room temperature so as to prepare DNA samples. The 10% native polyacrylamide gel electrophoresis (PAGE) was prepared by 5 × Tris–borate–EDTA (TBE) buffer. A loading sample was prepared by mixing 7 μL DNA sample, 1.5 μL 6 × loading buffer with 1.5 μL UltraPower dye, and then kept for 3 min so that the dye could integrate with DNA completely. The gel electrophoresis was run at 100 V for 60 min in 1 × TBE buffer which was running buffer. Then the polyacrylamide gel electrophoresis board was illuminated with UV light and scanned with a Molecular Imager Gel Doc XR (BIO-RAD, USA).

2.4. Preparation of epoxy group modified slide

The modification process of epoxy group on glass slides was performed according to the previous work [35]. The glass slides were first disposed by immersing them in basic piranha solution (40 mL of H_2O, 15 mL H_2O_2 and 15 mL of $NH_3 \cdot H_2O$) for 1 h at 60 °C, thoroughly washed by ultrapure water and dried. Then the waterless slides were immersed into ethyl alcohol solution containing 2% GOPS for 2 h at room temperature, thoroughly washed by ethyl alcohol and dried. GOPS was successfully coated on the slides to form the epoxy group modified slides. Finally, the prepared slides were pasted by perforating paper to form circular regions for future use.

2.5. Assembly of dendritic catalytic mimetic enzyme

All DNA were annealed by heating at 92 °C for 10 min and gradually cooling to room temperature. 10 μL NH_2-modified CP (1 μM) was dropt on slide overnight at room temperature and immobilized on slide by the reaction between epoxy group and amino group. The resulting slide was blocked with 10 μL PBS buffer for 2 h at room temperature. Following a washing step by Tris–HCl buffer, 5 μL TD of different concentrations, 5 μL H1 (10 μM), 5 μL H2 (10 μM) and 5 μL H3 (10 μM) were added onto the slide and incubated for 1 h at 37 °C. Subsequently, 2 μL FeTMPyP (10 μM) was injected into the mixture and incubated for 1 h at room temperature. After washed three times to remove the nonconjugated DNA and free FeTMPyP, the slide was successfully assembled with a dendritic catalytic DNA–FeTMPyP mimic enzyme.

2.6. Fluorescent measurement

1 μL H_2O_2 (400 mM), 1.4 μL tyramine (100 mM) and 7.6 μL Tris–HCl buffer were dropt onto the slide to incubate for 10 min at room temperature. After oxidation reaction, 8 μL of the mixture was added into 192 μL Tris–HCl buffer and mixed for fluorescent measurement. To evaluate the practicality of the proposed method in complex matrices, the recovery test was carried out by spiking standard target DNA solution (8 nM) into 10% (v/v) human serum sample.

3. Results and discussion

3.1. Characterization of dendritic DNA–porphyrin superstructure

Gel electrophoresis assay was operated to explore the self-assembly of dendritic DNA (Fig. 2A). A single band was individually shown in the positions corresponding to CP, TD, H1, H2 and H3 (lanes a–e). Mixing H1 and H2 at the same concentration, a new bright band appeared in the position corresponding to large molecular weight (lane f), which indicated most of H1 and H2 participated in forming H1–H2 duplex. When H3 was subsequently added, the bands at the position of low molecular weight disappeared (lane g), confirming H1, H2 and H3 were involved in the formation of H1–H2–H3. Incubating CP with TD of the same concentration, a single band corresponding to CP–TD was obtained (lane h). After H1 with 3-fold higher concentration than that of CP was injected, the CP–TD lane disappeared and new bands appeared at the positions corresponding to H1 and larger molecular weight, respectively (lane i), suggesting part of H1 was used to form CP–TD–H1. Upon the addition of H2, the H1 could be hybridized with two regions of H2 to form the linear H1–H2 duplex with some low molecular weight bands (lane j). The subsequent addition of H3 triggered another HCR with H1 and H2, and resulted in that the band tended to the large molecular weight position (lane k). Compared with lane j, the brightness in lane k was enhanced and some bands corresponding to lower molecular weight disappeared. The gel electrophoresis analysis identified that the assembly of dendritic DNA superstructure was feasible.

Besides, circular dichroism (CD) spectra were investigated to explore the interaction between FeTMPyP and dsDNA, and verified the formation of DNA–FeTMPyP (Fig. 2B). Free FeTMPyP did not show any obvious CD absorption (curve a). While the hybrid product of H1, H2 and H3 showed a positive peak and a negative peak in 280 and 245 nm, respectively (curve b), proving the formation of typical B-helix dsDNA [36]. After mixing dsDNA and FeTMPyP, CD absorption of dsDNA reduced and the peaks shifted (curve c), which demonstrated that FeTMPyP interacted with dsDNA by groove binding to form DNA–FeTMPyP. With the concentration of FeTMPyP increasing, the CD absorption continued to decrease (curve d) and it suggested that more groove sites of dsDNA were occupied by FeTMPyP molecules. The above results verified that dsDNA could be served as excellent carrier to gather FeTMPyP effectively.

3.2. Feasibility of this proposed method

The feasibility of this proposed method was verified by investigating fluorescence emission spectra under different conditions (Fig. 3). In the absence of FeTMPyP, the mixture of tyramine and H_2O_2 showed weak fluorescence intensity (curve a), which may be due to slight oxidation of tyramine in high concentration of H_2O_2. When TD was not involved in the assembly process of mimetic enzyme, few FeTMPyP could be absorbed on slide by electrostatic adsorption to result in a slight increase in fluorescence value (curve b). When TD was added, a short CP–TD duplex was formed and interacted with small amount of FeTMPyP, which caused the increase of the fluorescence value (curve c). Once TD, H1 and H2 were injected together, the fluorescence intensity was greatly improved by 38% comparing with that of CP–TD (curve d), suggesting linear dsDNA formed via HCR between H1 and H2 could gather lots of FeTMPyP molecules. Following the addition of H3, fluorescence intensity was further improved by 72% (curve e). The results indicated that the collaboration between TD with auxiliary DNAs could effectively extend the length of carrier for loading FeTMPyP to increase its catalytic capacity of dendritic DNA–FeTMPyP.

3.3. Optimization of conditions

Considering the important role of assembly time of dendritic DNA and substrate concentration in catalytic performance of DNA–FeTMPyP mimetic enzyme, incubation time of HCR and tyramine concentration were optimized (Fig. 4). The incubation time for HCR was monitored by fluorescence intensity (Fig. 4A). With the extending of incubation time, the fluorescence intensity increased, which indicated that more and more auxiliary DNAs were assembled onto the slide via HCR to construct the dendritic DNA superstructure. Then the fluorescence intensity reached a plateau after 60 min, suggesting the assembly was completed. Therefore, 60 min was chosen as the optimal HCR incubation time. On the other hand, tyramine concentration ranging from 0.49 mM to 1.40 mM was also optimized by the fluorescence intensity ratio

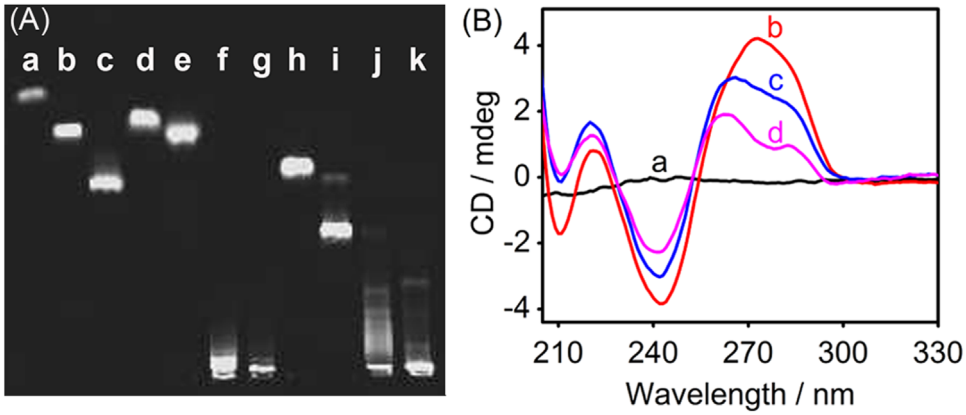

Fig. 2. (A) Gel electrophoresis images of CP (a), TD (b), H1 (c), H2 (d), H3 (e), H1+H2 (f), H1+H2+H3 (g), CP+TD (h), CP+TD+H1 (i), CP+TD+H1+H2 (j), CP+TD+H1+H2+H3 (k). The concentrations of CP, TD, H1, H2, H3 were 5, 5, 15, 15 and 15 μM, respectively. (B) CD spectra of 20 μM FeTMPyP (a), 2 μM H1–H2–H3 (b), 2 μM H1–H2–H3+20 μM FeTMPyP (c), 2 μM H1–H2–H3+60 μM FeTMPyP (d).

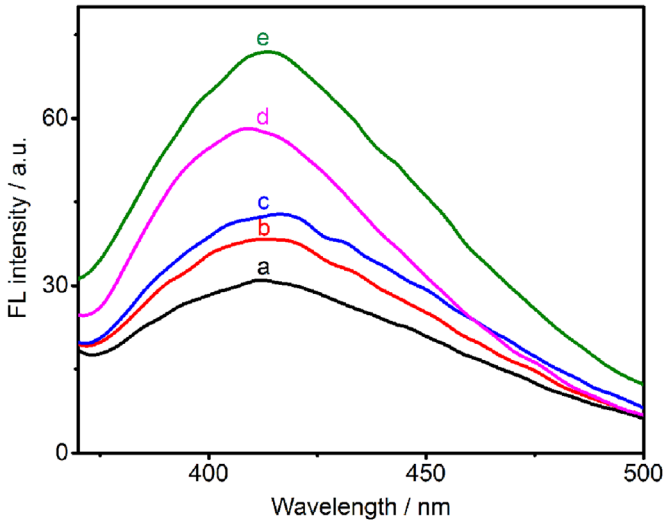

Fig. 3. Fluorescence emission spectra of oxidation product of tyramine oxidized by H_2O_2 (a), and catalyzed by FeTMPyP without TD (b), with TD (c), (c)+H1, H2 (d) and (d)+H3 (e) on CP modified slide in the presence of 40 mM H_2O_2. The concentrations of tyramine and TD were 0.7 mM and 8 nM, respectively.

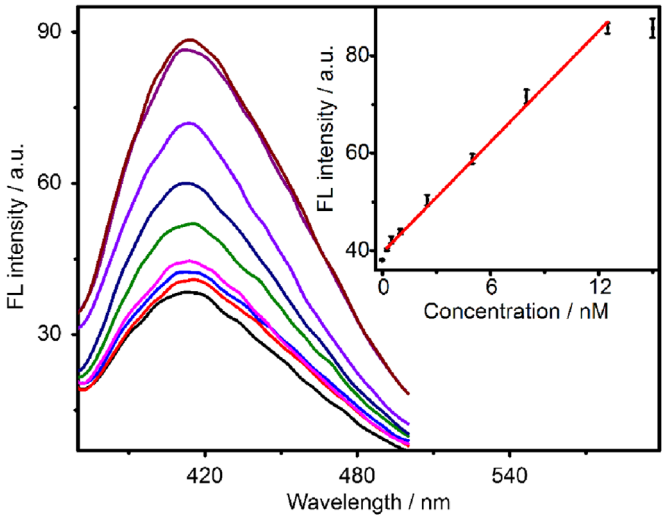

Fig. 5. Fluorescence spectra of the strategy based dendritic DNA–FeTMPyP as mimetic enzyme at 0, 0.25, 0.5, 1.0, 2.5, 5.0, 8.0, 12.5, 15 nM TD (from bottom to top). Inset: Calibration curve.

(Fig. 4B), F/F_0, where F and F_0 were fluorescence intensities in the presence and absence of the whole dendritic DNA, respectively. F/F_0 first increased and then decreased following the increase of concentration, and maximized at concentration of 0.7 mM. It could be explained that the lack of substrate limited the catalytic reaction, however, excess tyramine could improve F_0, due to the self-oxidation by H_2O_2. Hence 0.7 mM was chosen as the optimal substrate concentration for the following experiments.

3.4. DNA detection

Integrating HCR assembly with catalysis of FeTMPyP, a dendritic DNA–FeTMPyP mimetic enzyme was constructed and applied to fluorescent detection of DNA. As shown in Fig. 5, under the optimal detection conditions, the calibration plot showed a good linear relationship between the fluorescence intensity and target DNA concentration ranging from 0.25 to 12.5 nM. The linear regression equation was $I=39.61+3.78\times c$ ($R^2=0.996$), where I was the fluorescence intensity and c was TD concentration (Fig. 5, inset). The detection limit was calculated to be 103 pM, which was lower than or at least comparable to some of enzyme-assisted signal amplification detection methods [37,38] and much lower than nonenzyme-assisted fluorescent detection methods [39–41].

As comparison, a DNA sensing protocol was designed by measuring the fluorescence intensity of oxidation product of tyramine catalyzed by DNA–FeTMPyP in the absence of H3. The fluorescence intensity increased with the increasing TD concentration, and the plot of fluorescence intensity vs TD concentration showed a linear relationship in the concentration ranging from 0.5 to 12 nM ($R^2=0.997$). The detection limit was estimated at 3σ to be 402 pM (Fig. 6), which was about 4 times higher than that in the presence of H3. This result further identified that the dendritic DNA superstructure had the high capacity to load amounts of FeTMPyP for catalytically enhanced fluorescent detection.

3.5. Specificity of the catalytic fluorescence strategy

In order to study the specificity of the method, TD, single-base mismatched target (smT), three-base mismatched target (tmT) and non-complementary target (ncT) were measured (Fig. 7). The fluorescence intensity increment of TD was 2.8 times higher than that of smT, and 6.1 times higher than that of tmT. The intensity increment of ncT even in the 10-fold concentration was almost the same as blank. As a result, it suggested the proposed method possessed good specificity and could distinguish completely complementary DNA from smT.

In view of the practicability of the proposed method in complex

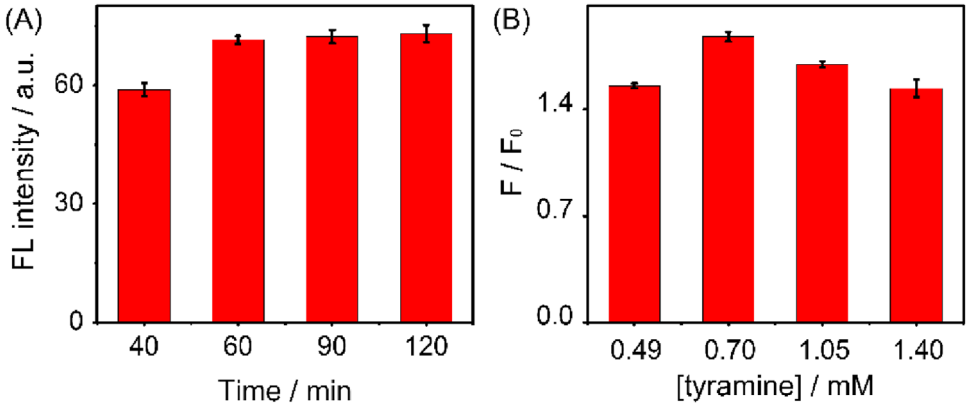

Fig. 4. Effects of (A) incubation time for HCR assembly on fluorescence intensity and (B) tyramine concentration on fluorescence ratio of F/F_0. F and F_0 were fluorescence intensities in the presence and absence of the whole dendritic DNA, respectively. The concentration of TD was 8 nM and the other parameters were under the optimal conditions.

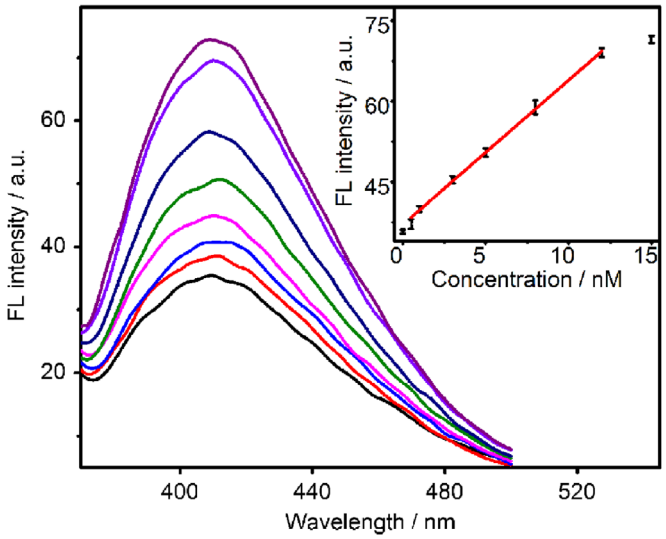

Fig. 6. Fluorescence spectra of the strategy based linear DNA–FeTMPyP with H1 and H2 at 0, 0.5, 1.0, 3.0, 5.0, 8.0, 12, 15 nM TD (from bottom to top). Inset: Calibration curve.

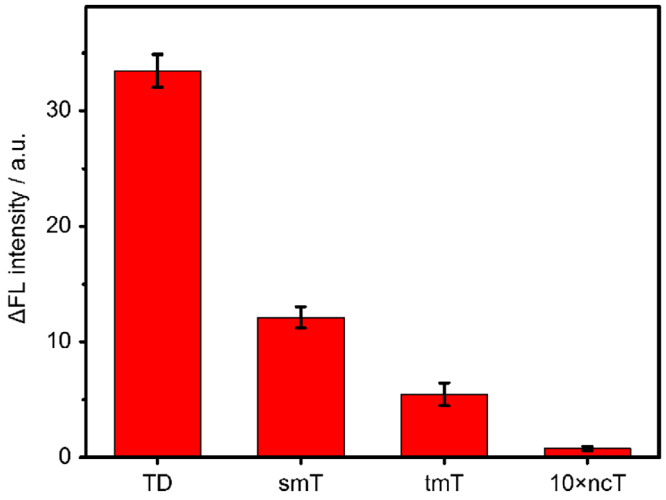

Fig. 7. Catalytic fluorescence intensity increment (ΔFL) of the strategy in the presence of TD (8 nM), smT (8 nM), tmT (8 nM) and ncT (80 nM) vs blank.

samples, it was used to detect TD in human serum samples. Three different serum samples were spiked with 8 nM TD for recovery experiment, and the recovery of the detection method were calculated to be 91.9 ± 1.1%, 95.5 ± 1.0% and 93.6 ± 1.1%, respectively, which indicated its good precision and acceptable reproducibility. Therefore, this catalytic fluorescence strategy could offer a practical and feasible way for quantitative detection of DNA in biological samples.

4. Conclusions

This work developed the dendritic DNA–FeTMPyP as enzymatic mimics for sensitive detection of DNA. The gigantic dendritic DNA could not only serve as the excellent carrier to enrich abundant FeTMPyP molecules, but also maintain the catalytic activity of FeTMPyP. Compared with harsh proteases, it owns excellent biomimetic catalytic activity with simpler preparation, easier modification and especially better stability. Therefore, employing dendritic DNA–FeTMPyP as a signal tag, a catalytically enhanced fluorescence strategy has been designed for the detection of DNA with high sensitivity, good specificity and practicability. This work not only provides a promising approach to build the dendritic DNA superstructure but also broadens the application of DNA–FeTMPyP mimetic enzyme in bioanalysis.

Acknowledgments

This research was financially supported by the National Natural Science Foundation of China (21375060, 21135002 and 21121091) and Priority Development Areas of the National Research Foundation for the Doctoral Program of Higher Education of China (20130091130005).

References

[1] R.M. Dirks, N.A. Pierce, Proc. Natl. Acad. Sci. USA 101 (2004) 15275–15278.
[2] G.Z. Zhu, S.F. Zhang, E.Q. Song, J. Zheng, R. Hu, X.H. Fang, W.H. Tan, Angew. Chem. Int. Ed. 52 (2013) 5490–5496.
[3] Q.G. Chen, Q.Q. Guo, Y. Chen, J. Pang, F.F. Fu, L.Q. Guo, Talanta 138 (2015) 15–19.
[4] S.Y. Niu, Y. Jiang, S.S. Zhang, Chem. Commun. 46 (2010) 3089–3091.
[5] L.J. Xiao, Y.Q. Chai, R. Yuan, Y.L. Cao, H.J. Wang, L.J. Bai, Talanta 115 (2013) 577–582.
[6] Y. Chen, J. Xu, J. Su, Y. Xiang, R. Yuan, Y.Q. Chai, Anal. Chem. 84 (2012) 7750–7755.
[7] L.J. Bai, Y.Q. Chai, R. Yuan, Y.L. Yuan, S.B. Xie, L.P. Jiang, Biosens. Bioelectron. 50 (2013) 325–330.
[8] J. Zhang, Y.Q. Chai, R. Yuan, Y.L. Yuan, L.J. Bai, S.B. Xie, L.P. Jiang, Analyst 138 (2013) 4558–4564.
[9] F. Xia, R.J. White, X.L. Zuo, A. Patterson, Y. Xiao, D. Kang, X. Gong, K.W. Plaxco, A. J. Heeger, J. Am. Chem. Soc. 132 (2010) 14346–14348.
[10] X. Chen, Y.-H. Lin, J. Li, L.-S. Lin, G.-N. Chen, H.-H. Yang, Chem. Commun. 47 (2011) 12116–12118.
[11] X. Chen, C.-Y. Hong, Y.-H. Lin, J.-H. Chen, G.-N. Chen, H.-H. Yang, Anal. Chem. 84 (2012) 8277–8283.
[12] T. Xue, S. Jiang, Y.Q. Qu, Q. Su, R. Cheng, S. Dubin, C.-Y. Chiu, R. Kaner, Y. Huang, X. F. Duan, Angew. Chem. Int. Ed. 51 (2012) 3822–3825.
[13] Q.B. Wang, J.P. Lei, S.Y. Deng, L. Zhang, H.X. Ju, Chem. Commun. 49 (2013) 916–918.
[14] H. Yamaguchi, K. Tsubouchi, K. Kawaguchi, E. Horita, A. Harada, Chem. Eur. J. 10 (2004) 6179–6186.
[15] J. Li, J.P. Lei, Q.B. Wang, P. Wang, H.X. Ju, Electrochim. Acta 83 (2012) 73–77.
[16] X.Q. Lu, F.P. Zhi, H. Shang, X.Y. Wang, Z.H. Xue, Electrochim. Acta 55 (2010) 3634–3642.
[17] A. Okunola, B. Kowalewska, M. Bron, P.J. Kulesza, W. Schuhmann, Electrochim. Acta 54 (2009) 1954–1960.
[18] R.F. Pasternack, E.J. Gibbs, J.J. Villafranca, Biochemistry 22 (1983) 2406–2414.
[19] R. Kuroda, H. Tanaka, J. Chem. Soc., Chem. Commun. (1994) 1575–1676.
[20] K.X. Wan, T. Shibue, M.L. Gross, J. Am. Chem. Soc. 122 (2000) 300–307.
[21] Y. Nitta, R. Kuroda, Biopolymers 81 (2006) 376–391.
[22] F. Wen, Y.H. Dong, L. Feng, S. Wang, S.C. Zhang, X.R. Zhang, Anal. Chem. 83 (2011) 1193–1196.
[23] T. Su, D. Zhang, Z. Tang, Q. Wu, Q.G. Wang, Chem. Commun. 49 (2013) 8033–8035.
[24] C. Wu, H.H. Sun, Y.F. Li, X.Y. Liu, X.Y. Du, X. Wang, P. Xu, Biosens. Bioelectron. 66 (2015) 350–355.
[25] Y.L. Cao, R. Yuan, Y.Q. Chai, L. Mao, H. Niu, H.J. Liu, Y. Zhuo, Biosens. Bioelectron. 31 (2012) 305–309.
[26] H. Chen, J.Q. Wang, G.H. Liang, P. Zhang, J.L. Kong, Chem. Commun. 48 (2012) 269–271.
[27] X.Q. Liu, R. Freeman, I. Willner, Chem. Eur. J. 18 (2012) 2207–2211.
[28] Q.F. Xu, A.P. Cao, L.F. Zhang, C.Y. Zhang, Anal. Chem. 84 (2012) 10845–10851.
[29] R.-M. Kong, X.B. Zhang, Z. Chen, H.M. Meng, Z.L. Song, W.H. Tan, G.L. Shen, R.Q. Yu, Anal. Chem. 83 (2011) 7603–7607.
[30] L.G. Xu, Y.Y. Zhu, W. Ma, H. Kuang, L.Q. Liu, L.B. Wang, C.L. Xu, J. Phys. Chem. C 115 (2011) 16315–16321.
[31] Y.Z. Xing, E.J. Cheng, Y. Yang, P. Chen, T. Zhang, Y.W. Sun, Z.Q. Yang, D.S. Liu, Adv. Mater. 23 (2011) 1117–1121.
[32] Y. Zang, J.P. Lei, P.H. Ling, H.X. Ju, Anal. Chem. 87 (2015) 5430–5436.
[33] Q.B. Wang, N. Xu, Z. Gui, J.L. Lei, H.X. Ju, F. Yan, Chem. Commun. 50 (2014) 15362–15365.
[34] Q.B. Wang, N. Xu, J.P. Lei, H.X. Ju, Chem. Commun. 50 (2014) 6714–6717.
[35] M. Vorlickova, I. Kejnovska, K. Bednarova, D. Renciuk, J. Kypr, Chirality 24 (2012) 691–698.
[36] A. Beloqui, J. Calvo, S. Serna, S. Yan, I.B.H. Wilson, M. Martin-Lomas, N.C. Reichardt, Angew. Chem. Int. Ed. 52 (2013) 7477–7481.
[37] L.B. Zhang, S.J. Guo, S.J. Dong, E.K. Wang, Anal. Chem. 84 (2012) 3568–3573.
[38] L.B. Zhang, J.B. Zhu, Z.X. Zhou, S.J. Guo, J. Li, S.J. Dong, E.K. Wang, Chem. Sci. 4 (2013) 4004–4010.
[39] X.Q. Liu, F.A. Wang, R. Aizen, O. Yehezkeli, I. Willner, J. Am. Chem. Soc. 135 (2013) 11832–11839.
[40] X. Zhu, H.Y. Zheng, X.F. Wei, Z.Y. Lin, L.H. Guo, B. Qiu, G.N. Chen, Chem. Commun. 49 (2013) 1276–1278.
[41] N. Enkin, F. Wang, E. Sharon, H.B. Albada, I. Willner, ACS Nano 8 (2014) 11666–11673.